Rare Metal Materials and Engineering
Volume 51, Issue 8, August 2022
Available online at www.rmme.ac.cn

Science Press

Cite this article as: Zhang Mao, Hu Changyi, Cai Hongzhong, et al. Microstructure and Properties of Nb-W Alloy Prepared via CVD[J]. Rare Metal Materials and Engineering, 2022, 51(08): 2830-2838.

ARTICLE

Microstructure and Properties of Nb-W Alloy Prepared via CVD

Zhang Mao, Hu Changyi, Cai Hongzhong, Wang Xian, Wei Yan

State Key Laboratory of Advanced Technologies for Comprehensive Utilization of Platinum Metals, Kunming Institute of Precious Metals, Kunming 650106, China

Abstract: Chemical vapor deposition (CVD) method was used to prepare Nb-W binary alloy. The microstructure and mechanical properties of the Nb-W binary alloy were studied by metallographic microscopy, scanning electron microscopy, electron probe spectroscopy and microhardness tests. Results show that the resulting Nb-W binary alloy has the characteristics of a regular angle layered structure, which is mainly composed of columnar crystals with the following composition fluctuations: Nb as the matrix at the connection between the layers with Nb-W solid solution distributed around it. The Nb-W solid solution is used as the matrix in the layer around which the Nb atoms are evenly distributed. Macroscopically, the W atoms mainly form a layer along the crystal growth direction, followed by transition to Nb atoms through the NbW solid solution; microscopically, the distribution of Nb and W atoms shows the characteristics of alternating content. The layered structure of the Nb-W alloy, composition difference between the layers, and overlapping difference of the grain size between the layers were verified by finite element simulation calculations and analysis, which play a significant role in improving the mechanical properties. The CVD forming mechanism and strengthening mechanism of Nb-W alloys were also revealed.

Key words: CVD; Nb-W alloys; layered structure; grain size; strengthening mechanism

The development of aerospace technology is inseparable from the improvement of the performance of high-temperature structural materials. The working environment of high temperature structural materials is extremely harsh with the gas intensity exceeding 2300 °C and heating rate reaching 3000 °C/s, and they are also subjected to strong gas erosion and ablation oxidation for long periods of time under the working conditions. Therefore, high temperature structural materials must have comprehensive performance characteristics, such as ultra-high temperature resistance, ablation resistance, erosion resistance, thermal shock resistance, oxidation resistance, high temperature gas sealing, low thermal conductivity, and light weight[1].

At present, candidate materials used or under development for ultra-high temperature structures mainly include carbon-based composites (carbon/carbon and carbon/silicon carbide) and refractory metals[2]. Carbon-based composites (carbon/carbon and carbon/silicon carbide) have excellent high temperature mechanical properties, such as high specific strength, high specific modulus, low density, low thermal expansion coefficient, corrosion resistance, and thermal shock resistance, which are considered to be the most promising high-temperature structural materials[3-5]. Thanks to the advent of carbon fiber, graphite continues to develop in the form of composite materials. Carbon matrix composites mainly include C/C and C/SiC composites, which are carbon fiber reinforced carbon matrix materials. In addition to the excellent properties of graphite, it is tougher and stronger than graphite, overcomes the crack sensitivity of graphite, and has good thermal shock resistance and performance designability. C/C composite material preforms include 2D, 3D, 4D, 5D, 7D, 11D, polar braiding, etc[6,7]. C/SiC composite material is a new type of ultra-high temperature thermal structural ceramic material developed in recent years. C/SiC composite materials use continuous carbon fiber as the reinforcement phase and silicon carbide and graphitized resin as the matrix, whose comprehensive mechanical properties and degree of densification are better than those of C/C composites. After

Recieved date: January 15, 2022
Foundation item: National Natural Science Foundation of China (51661014)
Corresponding author: Wei Yan, Ph. D., Professor, Kunming Institute of Precious Metals, Kunming 650106, P. R. China, E-mail: weiyan@ipm.com.cn

years of exploration and attempts, major breakthroughs have been made in the preparation process and application of carbon-based composite materials. Among them, Shanghai University and Central South University have made significant progress in the development of C/C composite materials. The C/SiC composite material developed by the National University of Defense Technology has been successfully used in liquid attitude control power systems. However, in the process of their development and use, it is found that some fundamental key problems of carbon-based composite materials have not been solved. The problem is mainly insufficient oxidation resistance; the common problem of carbon-based materials is poor oxidation resistance, which limits their application in oxidative environments. The air tightness is low due to the characteristics of the preparation process, in which high porosity is formed in the prepared carbon matrix composites (carbon/carbon, carbon/silicon carbide). For example, the open porosity in the SiC matrix can reach 10%~15%. Even if a densification treatment step is carried out, 3%~5% porosity is retained and high-pressure sealing cannot be achieved. The temperature resistance needs to be further improved. The melting point of the SiC reinforcing phase in the C/SiC composite material is 3000 °C. For applications above 2500 °C, its temperature resistance is obviously insufficient. Carbon-based composite materials (carbon/carbon and carbon/silicon carbide) are developed rapidly as new ultra-high temperature structural materials, but they cannot completely replace refractory metal alloys in terms of their processability, low plasticity, and compactness. Refractory metal materials have the characteristics of high melting point, ablation resistance, and good mechanical properties. They still have an irreplaceable role in the aerospace industry, atomic energy industry, metallurgical industry, chemical industry, and medical industry[8-10]. Therefore, refractory metal alloys will still occupy an important position in the future, even in the face of the challenges of carbon-based composite materials (carbon/carbon and carbon/silicon carbide). Among them, niobium and its alloys have excellent high temperature mechanical properties and good corrosion resistance with low density, high melting point, easy welding and forming, and good corrosion resistance. They still play an irreplaceable role in improving liquid rocket engine nozzle materials and replacing nickel-based superalloys as gas turbine and turbine blade materials[11]. Both niobium and tungsten have a body-centered cubic structures and a continuous solid solution can be formed between them, i.e., there is no intermediate phase in the entire composition range. The plastic transition temperature of niobium is extremely low and it has good room temperature processability and corrosion resistance. Tungsten has a very high melting point and shear modulus, and the addition of tungsten to niobium can improve the strength of niobium at room temperature and under high temperature conditions[12]. To date, the main application of niobium alloy is rocket propulsion[13]. C103 (Nb-Hf-Zr) niobium alloy has been used as a representative high temperature thermal structural material for the first generation of liquid rocket engine nozzles. Further improvement in the properties of C103 niobium alloy and the development of new alloy systems have always been an important direction during research on refractory metal materials. The working temperature of Nb521 (Nb-W-Mo-Zr) developed by the United States and Russia in the 1990s was increased to 1550 °C, which is a successful example of improving the properties of niobium alloys. Based on the aim of improving the thermal efficiency of thermal power plants and reducing carbon dioxide emissions, the Japan Institute of Ultra-High Temperature Materials has developed a niobium-based ultra-high temperature alloy to replace nickel-based superalloys for gas turbine blade materials, which increased the gas turbine inlet temperature to 1500 °C[14,15]. At present, China is carrying out research on the development of high-temperature oxidation and corrosion-resistant coatings. The Northwest Institute for Nonferrous Metal Research has carried out imitation research on C103 alloy, which has achieved great success in terms of the alloy composition, processing, coating, welding and non-destructive testing. The performance of the alloy has reached the level of similar alloys used in the United States[16]. A single-phase NbWHf superalloy material has been developed by Sha Jiangbo and others from Beihang University[17]. This superalloy material can surpass the room temperature plasticity that the current high-temperature material, NbWHfSi, with a two-phase Nb/Nb_5Si_3 structure cannot achieve, and has sufficient high temperature strength.

As one of the most important ultra-high temperature structural materials reported to date, Nb-W alloy has a very wide range of applications in high-tech fields, such as aerospace, aviation and atomic energy. The traditional methods used to prepare Nb-W alloys include casting and powder metallurgy methods, and the alloys are further strengthened by adding multiple components. In this study, chemical vapor deposition (CVD) technology was used to prepare Nb-W alloy for the first time and the microstructure and mechanical properties of the resulting Nb-W alloy were studied. The overlapping difference in the grain size between the layers was verified using finite element simulation calculations and analysis, which played a significant role in improving the mechanical properties. Our study has revealed the CVD forming mechanism and toughening mechanism of Nb-W alloys, explored and developed new preparation technologies for superalloy materials, and laid a theoretical foundation for the development of Nb-W binary alloys and other superalloy material systems with excellent mechanical properties, practical value, and technical foundations.

1 Experiment

1.1 Starting materials

The starting materials used to prepare Nb-W alloy via the CVD method were pure niobium sheets (purity>99.95%) and tungsten sheets (purity>99.95%) using Cl_2 (purity>99.6%) and H_2 (purity>99.95%) as the reactive gas. The base material was

metal molybdenum in the powder state suitable for metallurgy processing with a size of Φ35 mm×30 mm, and the surface of each matrix was treated in the same way to ensure the same surface state.

1.2 Experimental equipment

A schematic representation of the deposition of the Nb-W alloy coating on the molybdenum substrate is presented in Fig. 1. The deposition apparatus consists of a chlorination chamber, deposition chamber, heating system, and gas transport and vacuum system. The chlorination chamber and substrate after surface treatment were heated using an electric furnace and intermediate frequency induction furnace, respectively. The pressure of the deposition chamber was controlled using a vacuum pump and the flow rates of Cl_2 and H_2 were controlled independently using mass flow controllers.

The structure of the deposited layer was analyzed using a D/MAX-RC X-ray diffractometer (test conditions: Cu target, 40 kV, and 80 mA). The Nb-W alloy deposition layers were sampled, polished, and eroded for microstructure observation using a 4XC metallographic microscope. The surface morphology of the as-deposited layer was observed using a PHLIPS XL30 ESEM scanning electron microscope. A HXS-1000A digital microhardness tester was used to test the hardness of the platinum alloy samples (parameters: the indenter with a cone angle of 136° applied under a load of 0.1 kg onto the surface of the sample and maintained for 10 s prior to unloading). After the same sample was selected for multiple measurements at different positions, the maximum and minimum values were removed and the average value was recorded.

1.3 Experimental procedures

The whole system was evacuated and the vacuum state was maintained for 24 h to ensure the good sealing of the vacuum system. The substrate and metal starting materials (niobium and tungsten) were heated to the required temperature under a hydrogen gas atmosphere during the heating process. When the substrate and chlorination chamber reached the set temperature, purified and dried chlorine gas was introduced into the chlorination chamber and reacted with niobium and tungsten to generate niobium pentachloride ($NbCl_5$) and tungsten hexachloride (WCl_6). The gaseous $NbCl_5$ and WCl_6 were transported to the surface of the molybdenum substrate, which was inductively heated to a specified temperature and underwent a reduction reaction with hydrogen to deposit niobium and tungsten. The substrate was rotated to ensure the uniform thickness of the coating formed during the deposition process. The main chemical equations are shown below:

$$Nb(s)+2\frac{1}{2}Cl_2(g)\rightarrow NbCl_5(g) \quad (1)$$

$$W+3Cl_2(g)\rightarrow WCl_6(g) \quad (2)$$

$$NbCl_5(g)+2\frac{1}{2}H_2(g)\rightarrow Nb(s)+5HCl(g) \quad (3)$$

$$WCl_6(g)+3H_2(g)\rightarrow W(s)+6HCl(g) \quad (4)$$

$$H_2(g)+Cl_2(g)\rightarrow 2HCl(g) \quad (5)$$

The exhaust gas generated by the reaction was cooled and captured using liquid nitrogen in the filter bottle and then entered the mechanical pump discharge system.

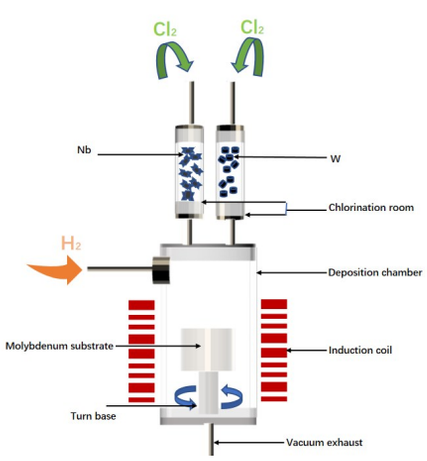

Fig.1 Schematic representation of the CVDNb/W apparatus

2 Results and Discussion

2.1 Microstructures of Nb/W alloys produced using CVD

In order to study the general microstructure of Nb/W alloys produced using CVD, a series of Nb-W alloys were prepared using different deposition parameters, as shown in Table 1. T_{Nb} and T_W represent the temperature at which the chlorination reaction of Nb and W occurs, respectively. T_{sub} is the deposition temperature. F_{Cl_2} and F_{H_2} represent the flow of chlorine and hydrogen.

Fig. 2 shows the metallographic microstructure of samples 1#, 2#, 3#, and 4#. Compared with Fig.2a and 2b, Fig.2c and 2d are significantly different, in which a layered structure is distributed perpendicular to the direction of the columnar crystals. There is no special structure in the metallographic microstructure of samples 1# and 2#, which may be due to the influence of the deposition parameters, leading to the very small mass percentage of W in the alloy, even lower than 1%, and the composition is almost close to single metal Nb from a macroscopic viewpoint. The resulting deposited microstructure is close to that of single metal Nb and does not exhibit a layered structure. Fig. 2c and 2d are the typical columnar

Table 1 Deposition parameters used for the preparation of Nb-W alloy sample

Sample	T_{Nb}/°C	T_w/°C	T_{sub}/°C	F_{Cl_2}(Nb)/mL·min^{-1}	F_{Cl_2}(W)/mL·min^{-1}	F_{H_2}/mL·min^{-1}
1#	300	550	1100	100	30	1000
2#	300	550	1100	200	60	1000
3#	300	600	1250	200	60	1000
4#	300	600	1250	250	60	1200

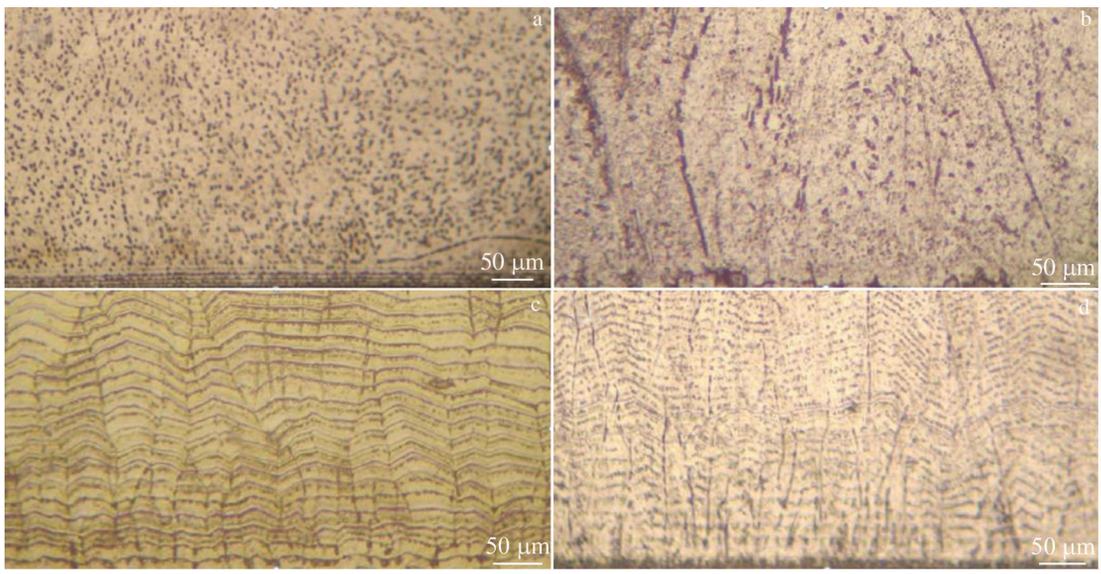

Fig.2 Metallographic microstructures of the as-prepared Nb-W alloy sample: (a) 1#, (b) 2#, (c) 3#, and (d) 4#

crystal structures of the Nb-W alloys. It is found that the niobium-tungsten alloy samples prepared via CVD have similar columnar crystal structures in Fig.2c and 2d, which are layered structures distributed perpendicular to the direction of the columnar crystals. Due to the change in the deposition parameters, the mass percentage of W in the samples 3# and 4# significantly increases and the presence of W affects the microstructure of the resulting Nb-W alloy, thus showing a special layered structure arranged layer by layer along the crystal growth direction, connecting at the grain boundary, but there is bending. According to the analysis of metallographic photographs and SEM images, the average layer thickness of all of the samples with layered structures is in the range of 10~15 μm. For the two samples with lower W contents and no layered structure, a few further studies are conducted, and the focus is on the group of samples with layered structures for further analysis.

Fig. 3 shows the electron channeling contrast (ECC) image of sample 4#. It can be seen that the same layered structural features as Fig. 2d appear in the microstructure. The layered structure is closely arranged and is naturally connected at the interface of the adjacent columnar grains without any obvious dislocation. The main advantage of ECC imaging is that it can reflect the atomic number contrast and crystal orientation contrast in the sample (atomic number contrast is dominant) [17,18]. The ECC image can directly reflect the fluctuation of the layered structure in the sample corresponding to the composition through the changes in the color depth, and grains with different brightness represent different grain orientations. The layered structure shows a change in the shade of color, as shown in Fig. 3. The darker areas observed at the interface indicate that the Nb content is higher and the lighter areas have a relatively low Nb content. The whole layered structure shows the alternating distribution of the Nb content from low to high and the W content from high to low. This shows that the layered structure is mainly related to the alloy composition of the deposited matrix.

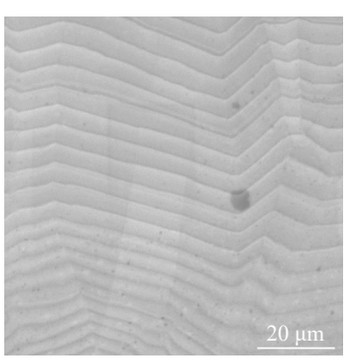

Fig.3 Image of the electron channeling contrast of sample 4#

Fig. 4 shows the element distribution of sample 4# by the electron probe composition. The upper images show the low-magnification image and the lower images are high-magnification image. Each image is divided into two parts: the left is the atomic number contrast image and the right is the corresponding compositional distribution map. The brown-yellow color represents Nb, dark blue represents W, and violet blue represents the (NbW) solid solution. At low-magnification, the distribution of Nb and W atoms is characterized by a gradual increase in the Nb content and a gradual decrease in the W content as the deposition process progresses. The general distribution trend shows that during the initial stage of growth, mainly W atoms (the right side is close to the substrate side) transform into a W-dominated (NbW) solid solution, and finally into a Nb-dominated (NbW) solid solution. The assumption that the layered structure is mainly related to the alloy composition of the deposited matrix in the above ECC image is verified. In the high magnification image, the interlayer Nb content is high and the

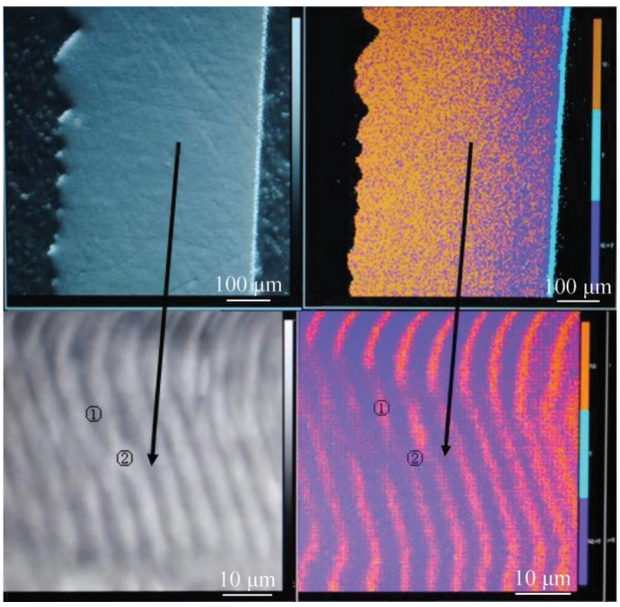

Fig.4 Element surface distribution in sample 4#

inner layer is a (NbW) solid solution by comparing the atomic number contrast map and corresponding surface distribution map, which is consistent with the analysis of the ECC images. Because a continuous solid solution is formed between Nb and W, there is no intermediate phase observed in the entire composition range, so the distribution of the solid solution phase and elemental phase of the Nb-W alloy can be judged by the distribution characteristics of the elements. If the interlayer is marked as ① and the inner layer is marked as ②, the distribution law of the layered structure is that ① and ② are periodically alternately arranged, and the corresponding phase distribution is characterized by the periodicity of Nb+(NbW) and (NbW)+Nb. The former means that it is based on Nb with (NbW) solid solution distributed, and the latter meant that it is based on a (NbW) solid solution with Nb distributed. Due to this undulating feature of the composition, there is a difference in the corrosion resistance between the layers, which in turn shows the layered structure in the metallographic corrosion photos.

To sum up, the distribution law of the constituent atoms of Nb-W alloy is as follows. Macroscopically, the W atoms mainly form a W layer along the crystal growth direction, which then transfrom to Nb atoms through the (NbW) solid solution; microscopically, the distribution of Nb and W atoms shows the characteristics of alternating content. Because Nb and W form a continuous solid solution, the changes in the macroscopic content is mainly realized by the change of the relative content of the two atoms in the solid solution.

2.2 Mechanical properties of Nb/W alloys produced by CVD

2.2.1 Intuitive analysis of grain size

The grain size was measured using metallographic photographs. Three different fields of view were selected for each sample, three line segments were taken for each field of view, and the average value was reported as the average grain size of the sample. The average grain size and related mechanical properties of each sample are listed in Table 2.

The average grain size, average strength of extension, fracture elongation, and microhardness of pure niobium and each sample are shown in Table 2. It can be seen that the average size of CVD niobium is 245 μm, the average grain size of CVDNb-W alloy prepared under different deposition parameters is in the range of 54~233 μm, and the average grain size of CVDNb-W alloy is reduced compared with niobium alloy. The W content is 0.68wt%, 0.79wt%, 8.50wt%, and 18.05wt% in sample 1#, 2#, 3#, and 4#, respectively, in which the increasing W content gradually decreases the average grain size of the sample, even down to several tens of micrometers. It can be seen that the introduction of W has a very significant refining effect on the niobium alloy grains. When the niobium-tungsten alloy is solidified, the tungsten atoms are segregated at the interface, and an increase in the supercooling during the crystallization process produces a great nucleation rate, in which the nucleation rate is much faster than the grain growth rate, providing enough time for the grains to grow. The niobium-tungsten alloy grains are therefore refined compared to niobium alloys. In addition, a large number of nucleation sites also hinder the growth of the grains, which is also the reason for promoting grain refinement[19,20].

2.2.2 Microhardness analysis

In samples 1#, 2#, 3#, and 4#, increasing the W content leads to increase in the microhardness. For samples 1# and 2#, the mass fraction of W are 0.68wt% and 0.79wt%, respectively, which are less than 1%. The composition is macroscopically close to single-metal Nb and the deposited microstructure is correspondingly close to single-metal Nb. There is no significant difference in microhardness when compared with CVD Nb. The deposited microstructure is also observed to be close to single metal Nb in the metallographic photographs (Fig. 2a and 2b). The mass fractions of W are

Table 2 Room temperature mechanical properties of Nb-W alloy prepared by CVD

Sample	Average grain size/μm	Strength of extension/MPa	Fracture elongation/%	Microhardness, HV/MPa	W content/wt%
CVD Nb	245	280	17.6	1019.2	0
1#	233	281	4.0	1029.0	0.68
2#	140	288	14.0	911.4	0.79
3#	115	350	5.4	1783.6	8.50
4#	54	403	10.0	2224.6	18.05

8.50wt% and 18.05wt% in samples 3# and 4#, respectively, which are all greater than 1%. W atoms have a significant impact on the microstructure of the Nb-W alloys (Fig. 2b and 2c). In the metallographic photographs, it is observed that the Nb-W alloy presents a layer-by-layer arrangement along the crystal growth direction of an orga-nized structure. Compared with niobium alloy microhardness (1019.2 MPa), the microhardness of sample 3# is 1783.6 MPa, which is increased by 75.0%. The microhardness of sample 4# is 2224.6 MPa, increased by 118.2%. This shows that an increase in the W content is the main reason for the increase in the microhardness of Nb-W alloy.

This can be mainly attributed to the phenomenon that the grains are refined due to the dissolution of the W atoms. The plastic deformation caused by the external force can be dispersed in more grains, the force is more uniform, and the stress concentration is small. In addition, the grain boundary area will increase during the grain refinement, and the grain boundary will be more tortuous, preventing the expansion of micro-cracks, thereby improving the hardness of the material macroscopically [21] .

2.2.3 Strength of extension analysis

The samples are processed into tensile specimens for tensile strength testing. The tensile members were all taken from the upper end face of the substrate, three selected for each sample, and the average tensile strength is reported as the tensile strength of the sample. It can be seen from Table 2 that in general, the tensile strength of Nb-W alloy increases with an increase in the W content, but the relationship between fracture elongation and alloy composition does not show a similar trend. It is worth noting that although the compositions of samples 1# and 2# are not very different and the tensile strength at room temperature is similar, the fracture elongation still shows a large difference. This indicates that the combination of different deposition parameters can deposit alloys with similar compositions, but different mechanical properties, i.e., the mechanical properties not only depend on the composition of the alloy, but are also affected by the deposition parameters used. When the mass fraction of tungsten is <1wt%, the properties of the alloy are not much different from those of pure metal Nb, and the strengthening effect becomes obvious when the mass fraction of tungsten is above 1wt%. Combining the average grain size data shown in Table 2, we can see that the average grain sizes of the four samples are 233, 149, 115, and 54 μm, respectively, i.e., the smaller the average grain size, the greater the tensile strength, but there is no such link for the fracture elongation.

The fracture morphologies of the four samples are shown in Fig. 5~8. It can be seen from Fig. 5 that the fracture surface morphology of sample 1# is mainly composed of multi-layer cleavage ladder accumulation and cracks occur at the grain boundary during fracture. The fracture mechanism is cleavage fracture and the macroscopic manifestation is brittle fracture. The fracture elongation is 4.0%. Fig. 6 shows that the fracture surface morphology of sample 2# is composed of dimples and river-like patterns. During the initial stage, cracks are generated at the grain boundary and then extended along the cleavage plane to form a river-like pattern. When the river-like pattern is developed to another grain boundary, part of it transforms into a dimple with plastic fracture characteristics. The fracture elongation of the sample is 14% and obvious necking phenomenon occurs during the stretching process. Fig. 7 shows that the fracture surface morphology of sample 3# is composed of a smooth fracture surface and river-like pattern cleavage surface. The fracture mechanism is mixed fracture and the fracture elongation is 5.4%. Fig. 8 shows that the fracture surface morphology of sample 4# is composed of a large number of river-like patterns, tearing edges, and some dimples. The macroscopic appearance is plastic fracture and the fracture elongation is 10%. In summary, when the Nb-W

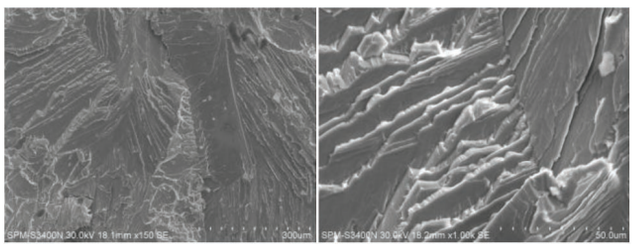

Fig.5 Fracture morphology of sample 1#

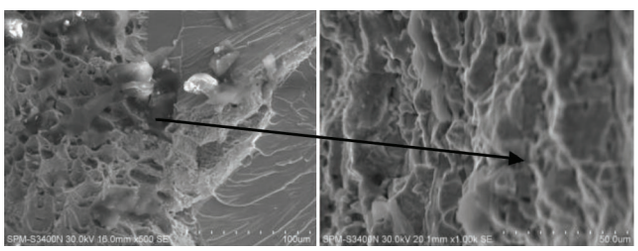

Fig.6 Fracture morphology of sample 2#

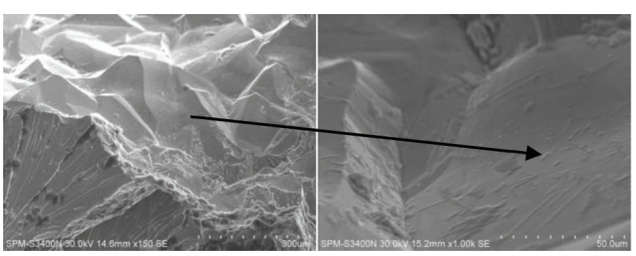

Fig.7 Fracture morphology of sample 3#

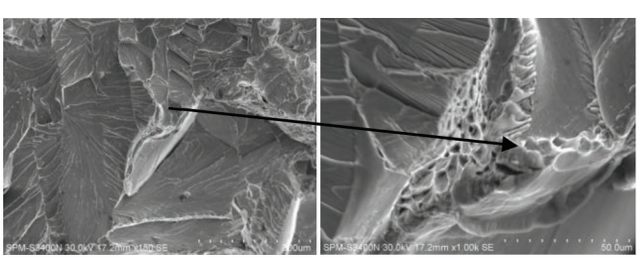

Fig.8 Fracture morphology of sample 4#

alloys are stretched, cracks often occur at the grain boundaries, but there are often multiple pathways in the process of crack propagation, i. e., there are intergranular fractures, cleavage fractures, and microporous polymerization on the microscopic level. The different proportions of the microscopic fracture mechanism show the different macroscopic fracture characteristics. In general, when the fracture surface morphology is composed of partial dimples, the fracture mechanism is close to plastic fracture (the fracture elongation is >5%). On the contrary, it is brittle fracture (fracture elongation is <5%).

2.3 Formation mechanism for the layered structure of CVDNb-W alloy

There are few reports on the preparation of alloys via CVD. At present, CVD basically uses the deposition of simple substances and compounds. It has been reported in Ref. [22] that a layered structure and composition fluctuations appear during the preparation of W-22wt% Re alloy using CVD and the fluctuation period is 1 μm, while the author did not give any explanation for this layered structure. The layered structure and compositional fluctuation characteristics of Nb-W alloy prepared via CVD in this paper are different from those reported in Ref. [22] in two main aspects: one is that the layer is thicker, reaching more than 10 μm and the other is that the layer is wavy, running through the entire sample (Fig. 2c and Fig. 3). While the layered structure reported in Ref. [18] is in the shape of a closing rhombus, which consists of relatively independent rhombus groups (Fig.9).

The CVD process of niobium-tungsten alloy is essentially a multiphase reaction at the gas-solid interface [23-25]. Various gas-phase chlorides of Nb and W pass through the gas boundary layer on the surface of the matrix via diffusion and viscous flow, and are adsorbed on the active sites on the substrate surface to chemically react with H_2 to generate Nb and W atoms. The Nb and W atoms then migrate through the surface, merge, nucleate, and grow into deposits. As far as the deposition process of Nb-W alloy is concerned, the preferentially adsorbed reactive gas will preferentially undergo a deposition reaction, [26] resulting in the micro-segregation of the components. During the competitive adsorption process of Nb and W chlorides at the same type of active sites on the surface of the substrate, the amount of adsorption is determined by the force between each component and the adsorption center, which is affected by the concentration of the components [27]. It can be seen from the elemental distribution map obtained during electron probe surface scanning spectroscopy shown in Fig.4 that W chloride is preferentially adsorbed on the surface of the molybdenum substrate, and W chloride is also preferentially reduced by H_2, thus forming the initial W layer. After the W layer is formed, the adsorption effect of tungsten chloride is stronger, further reduction reactions occur, and after a period of reaction consumption, the content of tungsten chloride in the deposition chamber decreases. At this time, the niobium chloride is enriched in the bottom layer of the boundary layer. The active center begins to be converted into the adsorption of niobium chloride under the action of concentration diffusion driving force. H_2 reacts with the enriched niobium chloride to generate Nb atoms and the existence of Nb atoms provides the basis for the further adsorption of niobium chloride, which promotes the reduction reaction of niobium chloride. The niobium chloride is consumed during the reduction reaction in the deposition chamber, tungsten chloride is gradually enriched again, and the adsorption of the active center is again dominated by tungsten chloride. The result of the above cyclic alternating reaction results in the formation of the Nb-W alloy layered structure. Therefore, the formation of the niobium-tungsten alloy layered structure is mainly the result of the combined effect of the adsorption characteristics and competing reactions of the surface process.

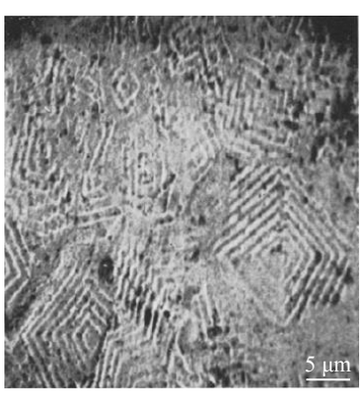

Fig.9 Segregated structure of W-Re alloy[22]

2.4 FEM establishment of the layered structure of CVDNb-W alloy

Using Nb, W, and Nb/W as the research objects, a finite element model (FEM) was established based on the finite element method and theory of structural mechanics. Static mechanical analysis of the material was carried out under certain constraints and loads. For static analysis, a three-point bending method was used to simulate the stress-strain experienced by the material during the bending process. Considering that the Nb/W sample obtained during the deposition experiment is small, the size selected for establishing the finite element model is 15 mm×3 mm×1 mm. At the same time, the analysis of the experimental samples shows that Nb and W exist in the form of layers, and the W content is in the range of 0.68%~18.05%. The established Nb/W composite material geometric model and finite element model are shown in Fig. 10. The material performance parameters are shown in Table 3.

In order to study the stress-strain of different materials under the same load, three-point bending simulations were carried out for the Nb, W, and Nb/W materials. A schematic representation of the loading is shown in Fig. 11 and Fig. 12, which show the strain conditions of the three materials under a load of 10 N. It can be seen that the maximum displacement of Nb, W, and Nb/W is 0.004 02, 0.001 05, and 0.001 45 mm, respectively (Fig. 12). The maximum displacement of the

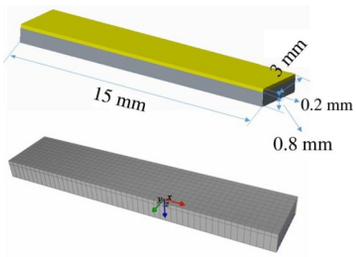

Fig.10 Geometric model and finite element model of the Nb/W composite

Table 3 Material performance parameters

Material	Elasticity modulus, *E*/GPa	Poisson' ratio, μ	Density/g·cm^{-3}
Nb	104	0.35	8.57
W	405	0.28	19.25

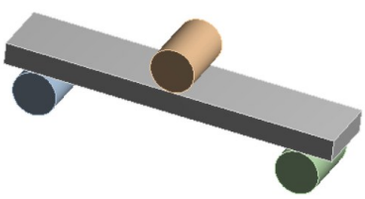

Fig.11 Schematic representation of three-point bending loading test

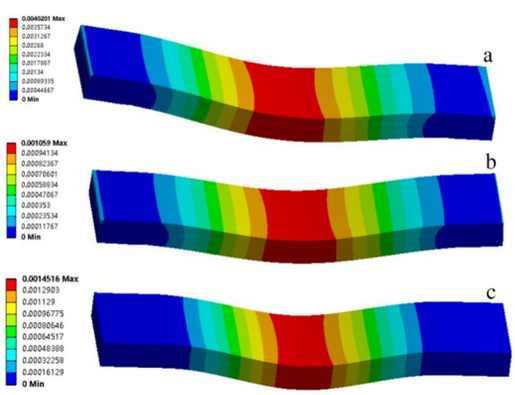

Fig.12 Displacement cloud diagram of Nb (a), W (b), and Nb/W (c) under the same load

layered conforming material lies between Nb and W. This shows that the stiffness of the Nb/W layered composite lies between Nb and W. The equivalent stress diagram of the three materials under the same load is shown in Fig. 13. It can be seen that the equivalent stress generated by the layered composite is the lowest under the same load, indicating that the composite material has better static mechanical advantages than the single pure metal. The layered structure of the Nb-W alloy, composition difference between the layers, and overlapping difference of the grain size between the layers are verified using finite element simulation calculations and analysis, which play a significant role in improving the

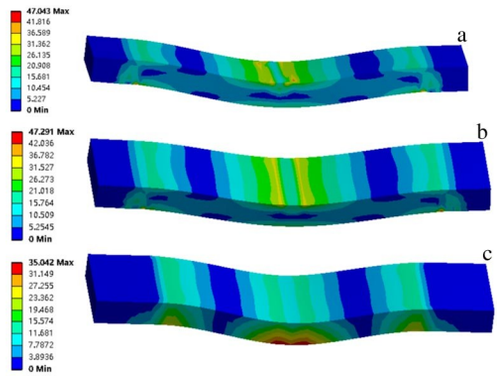

Fig.13 Equivalent stress diagram of Nb (a), W (b), and Nb/W (c) under the same load

mechanical properties. This calculation result is consistent with the mechanical property test experiments, which verify the mechanical property test and content analysis.

3 Conclusions

1) Nb-W binary alloy prepared via a CVD method has the characteristics of regular layered structure with composition fluctuations. The combination of different deposition parameters can prepare alloys with different compositions and mechanical properties.

2) With increasing W content, the average grain size of the sample gradually decreases, even down to several tens of micrometers. The introduction of W has a very significant refining effect on the niobium alloy grains.

3) The increasing W content can improve the microhardness of Nb-W alloy.

4) The formation of the niobium-tungsten alloy layered structure is mainly the combined effect of the adsorption characteristics and competing reactions in the surface process.

5) The composite material has better static mechanical advantages than the single pure metal. The layered structure of Nb-W alloy, composition difference between the layers, and overlapping difference in the grain size between the layers can be verified by finite element simulation calculations and analysis, which play a significant role in improving the mechanical properties.

References

1 Li Zhe, Wei Zhijun, Zhang Ping. *Proceedings of the 22nd Annual Meeting of Solid Rocket Propulsion of the Chinese Society of Astronautics in 2005 (Motor Volume)* [C]. Chengdu: Chinese Society of Astronautics, 2005

2 Liu Jun, Xiong Xiang, Wang Jianying *et al*. *Aerospace Materials & Technology*[J], 2005(1): 6 (in Chinese)

3 Buchanan F J, Little J A. *Corrosion Science*[J], 1993, 35: 1243

4 Hao W, Huang J F, Cao L Y *et al*. *J Alloys Compd*[J] 2014, 589: 153

5 Fu Q G, Li H J, Shi X H *et al*. *Appl Surf Sci*[J], 2006, 252: 3475

6 Chen Z F, Wu W P, Cheng H *et al*. *Acta Astronaut*[J], 2010, 66: 682

7 Wunder V, Popovska N, Wegner A *et al*. *Surf Coat Technol*[J], 1998, 100-101: 329

8 Han Xiufeng. *Thesis for Master*[D]. Xi'an: Northwestern Polytechnical University, 2006 (in Chinese)

9 Hu J D, Zuo X B, Feng Z *et al*. *Space Reentry and Remote Sensing*[J], 2011, 32(3) : 88

10 Huda Z, Edi P. *Materials & Design*[J], 2013, 46: 552

11 Harris B. *Physica Status Solidi*[J], 1968, 29(1): 383

12 The Writing Group of "Manual of Rare Metal Materials Processing". *Rare Metal Materials Processing Manual*[M]. Beijing: Metallurgical Industry Press, 1984: 261 (in Chinese)

13 Hebda J. *Thesis for Doctorate*[D]. El Paso: The University of Texas at El Paso, 2014

14 Zhang Xiaoming. *Rare Metal Letters*[J], 2005, 24(2): 3

15 Zhang Xiaoming, Tian Feng. *Rare Metal Letters*[J], 2007, 26(7): 12

16 Zhang Deyao, Zhao Tiefu, Fan Mingsheng *et al*. *Rare Metal Materials and Engineering*[J], 1977 (1): 30 (in Chinese)

17 Sha Jiangbo, Liu Dongming, Xu Huibin *et al*. *Chinese Patent*, 200510132598[P], 2005 (in Chinese)

18 Gutierrez-Urrutia I. *Microscopy and Microanalysis*[J], 2021: 1

19 Crimp M A. *Microscopy Research and Technique*[J], 2006, 69(5): 374

20 Li Xuming, Hu Changyi, Wei Yan *et al*. *Precious Metals*[J], 2019, 40 (S1): 44 (in Chinese)

21 Bruneton E, Tallaron C, Gras-Naulin A *et al*. *Carbon*[J], 2002, 40(11): 1919

22 Auck Y T, Byrne J G. *Journal of Materials Science*[J], 1973 (8): 559

23 Pierson H O. *Handbook of Chemical Vapor Deposition-Principles, Technology and Applications (2nd Edition)*[M]. New York: William Andrew Publishing, 1999

24 Choy K L. *Progress in Materials Science*[J], 2003, 48: 57

25 Hu Changyi, Li Jinghua. *Rare Metal*[J], 2001, 25(5): 364

26 Zhang Yingguang, Bai Xuefeng, Zhang Honglin *et al*. *Technology Forum*[J], 2005(12): 82

27 Ikeda S, Nagano M. *Reports of the Faculty of Science and Engineering*[J], 1984, 12

CVD制备Nb-W合金的显微组织和性能

张　茂，胡昌义，蔡宏中，王　献，魏　燕

(昆明贵金属研究所 稀贵金属综合利用新技术国家重点实验室，云南 昆明 650106)

摘　要：采用化学气相沉积（CVD）法制备Nb-W二元合金材料，通过金相显微镜、扫描电镜、电子探针和显微硬度仪研究了Nb-W二元合金的显微组织、力学性能。结果表明，CVD法制备的Nb-W二元合金具有规则角度层状结构特征，层状结构主要以柱状晶为主，并伴随着相应的成分起伏：层与层连接处以Nb为基体，周围分布有Nb-W固溶体，层内以Nb-W固溶体为基体，周围分布着Nb原子。宏观上在沿着晶体生长方向上开始基本以W原子为主形成一个W层，随后经过（NbW）固溶过渡到Nb原子；而微观上Nb和W原子的分布又显现出含量交替变化的特征。利用有限元模拟计算分析验证Nb-W合金材料的层状结构，以及层间的成分差异，发现层间晶粒尺寸的交叠差异对力学性能起到了明显的提升作用。揭示了Nb-W合金CVD成型机理与强化机制。

关键词：化学气相沉积（CVD）；Nb-W合金；层状结构；晶粒尺寸；强化机制

作者简介：张　茂，男，1997年生，硕士生，昆明贵金属研究所稀贵金属综合利用新技术国家重点实验室，云南 昆明 650106，E-mail：1808110235@qq.com